Biogeosciences Discuss., 10, 16329–16369, 2013
www.biogeosciences-discuss.net/10/16329/2013/
doi:10.5194/bgd-10-16329-2013

Biogeosciences
Discussions
Open Access

Exploring the response of West Siberian wetland methane emissions to future changes in climate, vegetation, and soil microbial communities

T. J. Bohn and D. P. Lettenmaier

Department of Civil and Environmental Engineering, University of Washington, Seattle, WA, USA

Received: 7 September 2013 – Accepted: 4 October 2013 – Published: 24 October 2013

Correspondence to: D. P. Lettenmaier (dennisl@uw.edu)

Published by Copernicus Publications on behalf of the European Geosciences Union.

Abstract

We ran the VIC land surface model over the West Siberian Lowland (WSL), forced with outputs from 32 CMIP5 models for the RCP4.5 scenario, and compared the effects of changes in climate and vegetation (leaf area index in particular) on predicted wetland CH_4 emissions and other fluxes for the period 2071–2100, relative to the period 1981–2010. We also explored possible responses of soil microbial communities to these changes. Our results suggest that, if soil microbial communities acclimatize to elevated temperatures without changes in species abundances, end-of-century CH_4 emissions from the WSL will only rise to $3.6\,\mathrm{Tg\,CH_4\,yr^{-1}}$ (6 % above historical emissions). In contrast, if microbial species abundances in the north additionally shift to resemble those in the south, CH_4 emissions will more than double, to $7.3\,\mathrm{Tg\,CH_4\,yr^{-1}}$. Crucially, while historical emissions were concentrated in the southern half of the domain, acclimatization plus microbial population shifts concentrate almost 3/4 of future emissions in the northern half of the domain, where the possible release of carbon with permafrost thaw is a concern. In addition, microbial population shifts disproportionately increase microbial activity in the period during and immediately following snowmelt, when highly labile carbon is first thought to be released from the soil. This work indicates the importance of better constraining the responses of soil microbial communities to changes in climate and vegetation as they are critical determinants of the region's future methane emissions.

1 Introduction

Global wetlands have been the subject of increased attention from the climate modeling community because their large, temperature-dependent methane (CH_4) emissions may provide a positive feedback to future warming (Melton et al., 2013; Eliseev et al., 2008; Gedney et al., 2004). Boreal and arctic wetlands are of particular concern, due to their large extent (Lehner and Döll, 2004), pronounced historic and projected climate warming at high latitudes (Serreze et al., 2000; Diffenbaugh and Giorgi, 2012) and the possibility that previously-frozen soil carbon will decompose (Koven et al., 2011; Schaefer et al., 2011; Walter et al., 2006; Zimov et al., 2006) or be exported to the Arctic Ocean (Raymond et al., 2007; Frey and Smith, 2005) as permafrost thaws. Despite its importance to the global carbon cycle, the response of northern wetland methane emissions to climate change is fraught with uncertainties due to uncertain projections of future climate and geographic distribution of vegetation, and the response of soil microbial communities to these changes.

Climate change can influence methane emissions directly through several mechanisms. Wetland CH_4 emissions have been observed to depend strongly on soil temperature and moisture conditions (Olefeldt et al., 2013; Limpens et al., 2008; Christensen et al., 2003; Saarnio et al., 1997; Dise et al., 1993). Model projections (IPCC, 2007) suggest that, by the end of this century, high-latitude annual temperatures will rise by 2.8–7.8 °C and annual precipitation will increase by 10–28 %; most global climate models agree that changes will be greater in winter than summer. But whether wetland soils become drier or wetter depends on the local trade-off between increased air temperature, and hence (in most climate models) increased evapotranspiration (ET) and water table drawdown; and increased precipitation, and hence shallower water tables (Bohn et al., 2007). In addition, warmer conditions and greater atmospheric CO_2 concentrations can be expected to lead to greater net primary productivity (NPP) (Wania et al., 2009), thereby supplying more labile carbon substrate for the production of methane (via root exudates, Riley et al., 2011; Walter and Heimann, 2000). If the drying is sufficiently large, the net wetland response to warming can be a reduction in methane emissions, leading to a negative climate-wetland CH_4 feedback (Ringeval et al., 2011).

In response to these changes in climate, dynamic global vegetation models (DGVMs) generally have predicted a northward shift in the geographic ranges of boreal and arctic biomes by the end of this century, with forests displacing tundra and, within tundra, taller shrublands displacing prostrate shrub tundra (Kaplan and New, 2006; Alo and Wang, 2008a; Jiang et al., 2012; Sitch et al., 2008), resulting in a corresponding increase in average leaf area index (LAI) between 1 and 4 $m^2 m^{-2}$ throughout most of the high latitudes (Alo and Wang, 2008a, b). Assuming these changes apply equally to wetland vascular plants, this could have multiple effects on wetland carbon cycling. First, greater LAI could lead to further increases in NPP (Alo and Wang, 2008a), providing more labile carbon to the soil via root exudates (a positive feedback, Riley et al., 2011). Second, greater LAI could lead to further increases in ET (Alo and Wang, 2008b), potentially increasing the negative feedback on wetland greenhouse gas emissions (Ringeval et al., 2011). Thus, increases in LAI bring another set of trade-offs between NPP and ET. Third, the distribution of plants with aerenchyma (a conduit of both CH_4 to the atmosphere and oxygen to the root zone) may change, affecting the relative strengths of different pathways of methane to the atmosphere (Riley et al., 2011; Berrittella and van Huissteden, 2011; Christensen et al., 2004).

Not only do uncertainties in future climate and vegetation distributions lead to uncertainties in future ambient soil conditions, but the possible responses of soil microbial communities to these long-term changes are also poorly known (Graham et al., 2012; Conant et al., 2011). Some evidence exists for acclimatization (reduction in response over time) to elevated temperatures (Allison et al., 2010). However, the underlying mechanism for this has not been determined conclusively, and not all studies agree (e.g., Contosta et al., 2013). Another potential microbial response is the shifting of species abundances as local climate conditions and vegetation change. It has been noted that most species of microbes have essentially global geographic distributions (Finlay and Clarke, 1999), due to their ease of geographic dispersal (e.g., airborne dispersal; DeLeon-Rodriguez et al., 2013). Indeed, evidence from temperate bogs and elsewhere suggests that differences in microbial community composition over large geographic areas depend more on local environmental conditions than on the distance between them, implying that dispersal has not encountered a major barrier (Yavitt et al., 2012; Dumbrell et al., 2010). Similarly, there is evidence of a strong correlation between the strength of CH_4 emissions and plant species assemblages in peatlands across the UK (Levy et al., 2012), the pan-Arctic (Olefeldt et al., 2013) and the West Siberian

Lowland (Glagolev et al., 2011). Furthermore, field and laboratory studies indicate a statistically significant difference between the responses of soil microbial communities to temperature (Q10 parameter values) of sphagnum-dominated wetlands and sedge-dominated wetlands (Lupascu et al., 2012). Taken together, these findings suggest that, as vegetation patterns shift, species abundances in microbial communities might shift with them (albeit not all at the same rates; Pickles et al., 2012). Whether these shifts will replicate the plant and microbial assemblages (and their characteristic responses to soil conditions) from the south to the north or create entirely new assemblages (and new responses to soil conditions) is an open question.

Various individual aspects of the influence of vegetation distribution and soil microbial responses at large scales have been explored (Ringeval et al., 2011; Koven et al., 2011; Riley et al., 2011; Berrittella and van Huissteden, 2011) but, to our knowledge, no large-scale modeling studies have considered the effects of microbial population shifts on future land surface methane emissions. This is due in part to the application of a single set of methane emissions parameters across large portions of the globe in most studies (Bohn et al., 2013b). Similarly, no studies have compared the relative magnitudes of climate-, vegetation-, and soil microbe-based uncertainties in methane emissions.

The West Siberian Lowland (WSL) provides an interesting arena for testing the possible effects of microbial acclimatization and population shifts, in conjunction with changes in climate and vegetation. Intensive observations over a 2000 km transect of the region (Glagolev et al., 2011) demonstrated that the eutrophic mires in the south of the region emit substantially more methane per unit area than the tundra wetlands in the north. Bohn et al. (2013b) applied the methane emissions model of Walter and Heimann (2000) to the WSL and found little overlap between the likely Q10 parameter values in the northern and southern wetlands. While other factors also might have played a role, these results imply substantially different responses to climate change between the two subregions' plant and microbial communities. Thus, in the WSL, a northward shift in vegetation and microbial communities might bring with it a northward shift in the response to climate change, resulting in an additional increase in methane emissions. In contrast, acclimatization might be expected to reduce the response of methane emissions to climate change.

In this study we attempt to determine the range of possible end-of-century methane emissions from the WSL, characterize the dominant factors (climate, vegetation, microbial response) that influence them, and identify the mechanisms by which they act, including trade-offs between them. To this end, we ran the Variable Infiltration Capacity (VIC) land surface model (Liang et al., 1994), linked to the wetland methane emissions model of Walter and Heimann (2000), forced in off-line simulations with the outputs of CMIP5 21st century climate projections (Taylor, et al., 2012) for the RCP 4.5 pathway (essentially a middle-of-the-road future scenario for global greenhouse gas emissions).

2 Methods

2.1 Study domain

The West Siberian Lowland (WSL; Fig. 1a) which includes approximately 800 000 km^2 of lakes and wetlands, is the largest high-latitude wetland region in the world (Kremenetski et al., 2003; Sheng et al., 2004; Peregon et al., 2009). Spanning 18° of latitude (55–73° N) from the Eurasian Steppe to the Arctic Ocean, the WSL contains both permafrost and permafrost-free wetlands (Fig. 1a). These lakes and wetlands are interspersed with boreal forest (taiga) in the south and tundra in the north. Leaf Area Index (LAI) values derived from MODIS imagery (Myneni et al., 2002) vary accordingly from south to north, with values (one-sided and/or projected) ranging from 3 to 5 in the taiga declining northward to the treeless tundra above 70° N (Fig. 1b).

2.2 Model formulation and parameter values

Our study builds on the historical simulations of Bohn et al. (2013b) and uses the model formulation described therein. That study used a modified version of the Variable Infiltration Capacity model (VIC; Liang et al., 1994) land surface model, release 4.1.2. VIC 4.1.2 contains a frozen soil physics model (Adam and Lettenmaier, 2008; Cherkauer and Lettenmaier, 1999) and a dynamic lake-wetland model (Bowling and Lettenmaier, 2010). As described in Bohn et al. (2013b), VIC 4.1.2 was extended to include a distributed water table depth (WTD) scheme that accounts for wetland microtopography, such that wetlands contain a time-varying inundated area fraction A_{inund} (where standing water exists above the soil surface) which is a subset of a time-varying saturated area fraction Asat (where the water table is at or above the soil surface). Another modification to VIC 4.1.2 included formulations for carbon cycle processes such as NPP and aerobic soil respiration (Rh), both of which are inhibited under saturated conditions (Bohn et al., 2013b). Additionally, the version of VIC 4.1.2 we used was coupled to the wetland CH_4 emissions model of Walter and Heimann (2000). As in Bohn et al. (2013b), all carbon fluxes were computed at several points along each grid cell's water table distribution and integrated to account for the net effect of fractional saturation on the cell's carbon fluxes.

Model parameter values were taken from Bohn et al. (2013b). As in Bohn et al. (2013b), wetland fractional areas were derived primarily from Sheng et al. (2004). Monthly historical wetland LAI values were computed as the average MODIS (Myneni et al., 2002) LAI value for all pixels that fell within the wetland portion of each grid cell.

For those parameters that were calibrated, we used the median values from Bohn et al. (2013b). In that study, parameters for the wetland methane emissions model were calibrated to match the in situ observations of Glagolev et al. (2011). Because wetlands in the southern half of the domain are much more productive than those in the northern half of the domain, we used separate CH_4 parameter values in the southern and northern halves, with the geographic boundary at approximately 62° N (denoted in Fig. 1b), corresponding to northern boundary of the Middle Taiga zone (Glaglolev et al., 2011). The primary difference between the two parameter sets was the range of values for rq10 (which governs methanogenesis temperature sensitivity as in Walter and Heimann, 2000), which ranged from 9.7 to 11.7 (median 10.7, unitless) in the south and from 2.5 to 5.2 (median 3.4) in the north. This difference is consistent with the variability in observed Q10 values throughout the high latitudes (Lupascu et al., 2012). The values used in this study for these methane emissions model parameters are listed in Table 1.

2.3 Meteorological forcings

Meteorological forcings were derived for the periods 1948–2010 (historical) and 2011–2100 (future). VIC requires hourly values of air temperature, precipitation, wind speed, humidity, shortwave and longwave radiation, and atmospheric CO_2 concentration as inputs. We used methods described in Bohn et al. (2013a) to derive hourly values of all of these variables (except CO_2) from daily values of precipitation, minimum and maximum temperature, and wind speed. Historical observations of these daily variables were derived over the 100 km EASE polar azimuthal equal-area grid (Brodzik and Knowles, 2002) from a combination of the daily meteorological fields of Sheffield et al. (2006) and gridded monthly observations (Willmott and Matsuura, 2001; Mitchell and Jones, 2005) via the methods of Adam and Lettenmaier (2003) and Adam et al. (2006). Future values of these variables were derived from model projections from the fifth phase of the Coupled Model Intercomparison Project (CMIP5, Taylor et al., 2012), for the Integrated Assessment Modeling Consortium (IAMC) RCP4.5 scenario (Moss et al., 2010) via what is commonly termed the “delta” approach (Hamlet and Lettenmaier, 1999). In the delta approach, fractional changes in monthly precipitation (future/historic) and differences in monthly average temperature are applied, on a fixed seasonal cycle, to historic observations to form future scenarios. In our implementation, for each grid cell and each of 32 CMIP5 models (listed in Table 2), we computed a long-term climate trajectory from the 31 yr moving average of monthly air temperature and precipitation for the years 2010–2100 (from the CMIP5 projections), assigned to the year at center of window. We then converted these time series into monthly additive (temperature) or multiplicative (precipitation) anomalies relative to the model’s local mean over the historical scenario for the period 1975–2005 (because CMIP5 historical simulations end at year 2005). These anomalies were then regridded to the 100 km EASE grid. For each year in this time series, we then applied that year's monthly temperature and precipitation anomalies to one year of the historical daily forcings described above, randomly sampled from the period 1980–2010. For atmospheric CO_2 concentrations, we used the CMIP5 ensemble mean values.

2.4 Changes in LAI

Many CMIP5 models contained a dynamic vegetation component (Table 2) and predicted changes in the geographic distribution of vegetation over the next century. To account for the effects of these changes on LAI and consequently on carbon fluxes (NPP, RH, CH_4) as well as hydrology (ET, saturated area, water table depth), we converted each model's predicted end-of-21st-century (whole-gridcell) LAI to an equivalent end-of-century VIC (wetland) LAI via quantile mapping (Panofsky and Brier, 1968), under the assumption that the afforestation predicted by each dynamic vegetation model for the entire grid cell will apply in wetlands, too, relative to their own distribution of LAI. For each CMIP5 projection with a DGVM, we computed the percentile of each EASE-grid cell's wetland average LAI with respect to all the cells in the domain, for two periods: historical (1981–2010) and future (2071–2100). Similarly, we computed the percentile of each grid cell's average present-day wetland LAI as given by MODIS with respect to all cells. Then, for each CMIP projection, we mapped the CMIP5 historical and future LAI values to the corresponding MODIS LAI value of the corresponding percentile of the MODIS LAI distribution. The difference between these two MODIS LAI values was then added to the present-day MODIS LAI value as an estimate of the future wetland-average LAI for the grid cell. Grid cells for which the future CMIP5 LAI had no present-day analog were assigned the average change in LAI of their neighbors. No other vegetation-specific parameters were changed.

2.5 Simulations

To investigate the effects of changes in temperature, soil moisture, and LAI separately and in combination, we performed several sets of simulations (listed in Table 3). "Warming + Drying + LAI" consisted of 32 separate simulations, one per CMIP5 model, using the model's meteorological outputs and either the model's predicted LAI, if the model contained a dynamic vegetation component, or (for models without a DGVM), the median LAI of the models with DGVMs, to force our modified VIC LSM. "Warming + Drying" was the same as Warming + Drying + LAI, but held the seasonal cycle of LAI constant at historical MODIS values. Similarly, "Warming + LAI" was the same as Warming + Drying + LAI but with Asat and WTD in our LSM prescribed by repeating their daily values over the period 1981–2010 for the three 30 yr periods 2011–2040, 2041–2070, and 2071–2100. Finally, "Warming" prescribed the historical values of LAI, Asat, and WTD. All simulations used the final state of the historical simulation of Bohn et al. (2013b) as the initial state of our LSM runs.

To bracket the range of possible responses of soil microbial communities to changes in ambient soil conditions, we performed three variations of each of the above simulations (Table 4): one without acclimatization or population shifts ("NoAcc + NoShift"), one with acclimatization ("Acc + NoShift"), and one with both acclimatization and population shifts ("Acc + Shift"). Acclimatization was modeled by replacing the constant Tmean parameter in the methane emissions model (Walter and Heimann, 2000) with the 10 yr moving average of the vertically-averaged temperature in the top 1 m of the soil column. Population shifts were modeled as a complete replacement of northern microbial species abundances with those of the south. Accordingly, we replaced all instances of the northern values of the methane emissions parameters r0, xvmax, rkm, rq10, and oxq10 with their southern counterparts.

3 Results

3.1 Future climate and LAI

Because the majority of carbon fluxes take place in the WSL during the summer months (June–August), we focused our analysis on summer climate and LAI values. Changes over the 21st century in summer air temperature (ΔT_{JJA}) and summer precipitation (ΔP_{JJA}) predicted by the CMIP5 models are plotted in Fig. 2 for the southern (south of 62° N) and northern (north of 62° N) halves of the domain (Fig. 2a and b, respectively). Predicted increases in summer air temperature (ΔT_{JJA}) were similar over the two halves of the domain, ranging from 1 to 5 °C (median approximately 3 °C) with the exception of one model (GFDL-ESM2M) predicting essentially no change in summer temperature in the south. In contrast, predicted changes in summer precipitation (ΔP_{JJA}) were more negative in the south (−19.6 % to +29.1 %, with a median of 0.0 %) than in the north (−7.2 % to +22.6 %, with a median of +7.7 %). In the south, ΔT_{JJA} and ΔP_{JJA} were moderately negatively correlated (Pearson's r of −0.53).

Profiles of JJA LAI ($\mathrm{LAI}_{\mathrm{JJA}}$) values for CMIP5 models (whole-gridcell) and VIC (wetland only) are shown in Fig. 3. The original CMIP5 historical $\mathrm{LAI}_{\mathrm{JJA}}$ values (Fig. 3a) displayed a large degree of scatter, especially north of 60° N. The median $\mathrm{LAI}_{\mathrm{JJA}}$ peaked at approximately 3 $\mathrm{m^2\,m^{-2}}$ between 58 and 60° N and declined to the north. Among the CMIP5 models, projected 21st century changes in $\mathrm{LAI}_{\mathrm{JJA}}$ ($\Delta\mathrm{LAI}_{\mathrm{JJA}}$) were positive everywhere (median of approximately 0.5 $\mathrm{m^2\,m^{-2}}$) and only exceeded 1 $\mathrm{m^2\,m^{-2}}$ at the 75th percentile or higher (Fig. 3b). Uncertainty in $\Delta\mathrm{LAI}_{\mathrm{JJA}}$ increased from south to north, as a result of disagreement among models about the amount of northward expansion of the boreal forest. The resulting end-of-century $\mathrm{LAI}_{\mathrm{JJA}}$ values (Fig. 3c) displayed greater uncertainty north of 60° N than their historical values.

Historical MODIS wetland $\mathrm{LAI}_{\mathrm{JJA}}$ values (Fig. 3d) also peaked at 3 $\mathrm{m^2\,m^{-2}}$ at 56° N and declined northward, but tended to fall 0.5–1 $\mathrm{m^2\,m^{-2}}$ below the median historical CMIP5 $\mathrm{LAI}_{\mathrm{JJA}}$ values in the northern half of the domain. The values of $\Delta\mathrm{LAI}_{\mathrm{JJA}}$ derived from quantile mapping (Fig. 3e) were broadly similar to the $\Delta\mathrm{LAI}_{\mathrm{JJA}}$ values from the individual CMIP5 models (Fig. 3b), with the exception of lower variability in the highest percentiles. Similar to the CMIP5 values, the end-of-century VIC wetland $\mathrm{LAI}_{\mathrm{JJA}}$ values (Fig. 3f) displayed more uncertainty in the north (1–2 $\mathrm{m}^2\,\mathrm{m}^{-2}$, or approximately 50–200 % of the median values) than the south (1 $\mathrm{m}^2\,\mathrm{m}^{-2}$, or 30–50 % of the median values). But at all latitudes the uncertainty in VIC $\mathrm{LAI}_{\mathrm{JJA}}$ values was less than half that of the CMIP5 models, due to our application of the $\Delta\mathrm{LAI}_{\mathrm{JJA}}$ values to a single set of historical (MODIS) values. Spatial average $\Delta\mathrm{LAI}_{\mathrm{JJA}}$ was moderately correlated with ΔT_{JJA} in both the southern ($\rho = 0.67$) and northern ($\rho = 0.56$) halves of the domain.

3.2 Effects of changes in climate and LAI

Our results (summarized in Fig. 4, for the NoAcc + NoShift case, and in Table 5) indicated that, for the most important greenhouse fluxes, warming will act in opposition to drying and increasing LAI. In the Warming simulation (blue bars in Fig. 4), LAI, summer saturated area ($\mathrm{Asat}_{\mathrm{JJA}}$) and water table depth ($\mathrm{WTD}_{\mathrm{JJA}}$) were all prescribed at historical values (Fig. 4a and b). This resulted in substantial increases in NPP, Rh, and especially CH_4 fluxes (end-of-century totals over the WSL of 199 $\mathrm{Tg\,C\,yr}^{-1}$, 191 $\mathrm{Tg\,C\,yr}^{-1}$, and 7.80 $\mathrm{Tg\,CH_4\,yr}^{-1}$, respectively; Fig. 4c–e). Because Rh is more sensitive to temperature than NPP in our model (see Bohn et al., 2013b for parameter values), Rh increased faster than NPP, increasing the net flux of carbon to the atmosphere (Cnet; negative of carbon uptake) from its historical value of −14 $\mathrm{Tg\,C\,yr}^{-1}$ to just −2.2 $\mathrm{Tg\,C\,yr}^{-1}$ (Fig. 4f). The large increase in CH_4 emissions and reduced carbon uptake drove a large increase in greenhouse warming potential (GHWP) emissions from 12 to 135 $\mathrm{Tg\,CO_2\,yr}^{-1}$ (Fig. 4g). Most terms responded similarly in the south and north halves of the domain; exceptions are investigated in Sect. 3.4. Thus, warming alone resulted in large increases in net fluxes to the atmosphere.

Increasing LAI (without drying) reduced net fluxes to the atmosphere, despite causing increases in individual fluxes. In the Warming + LAI simulation (green bars), end-of-century NPP rose to 240 $\mathrm{Tg\,C\,yr^{-1}}$ (due to larger photosynthesizing area), and Rh rose to 2910 $\mathrm{g\,C\,yr^{-1}}$ (due to more carbon substrate entering the soil). Because NPP is more sensitive to LAI than Rh over decadal time scales, NPP increased more than Rh, causing carbon uptake to surpass historical levels (Cnet of −22 $\mathrm{Tg\,C\,yr^{-1}}$, Fig. 4f), and reducing GHWP to 66 $\mathrm{Tg\,CO_2\,yr^{-1}}$ (Fig. 4g). $\mathrm{CH_4}$ was relatively insensitive to increased LAI.

Climate-induced drying (Warming + Drying; yellow bars) also acted in opposition to warming alone. In this simulation, the summer saturated area as a fraction of wetland area, $\mathrm{Asat_{JJA}}$ (Fig. 4a) decreased from 0.46 to 0.42, and $\mathrm{WTD_{JJA}}$ (Fig. 4b) increased from 17 to 20 cm. The reduction of saturated area led to increases in NPP and Rh (to 220 and 210 $\mathrm{Tg\,C\,yr^{-1}}$, respectively) relative to warming alone, due to their inhibition under saturated conditions (Fig. 4c and d). In contrast, the drier soils yielded a smaller end-of-century $\mathrm{CH_4}$ flux (7.2 $\mathrm{Tg\,CH_4\,yr^{-1}}$) than for warming alone (Fig. 4e). Carbon uptake increased (Cnet decreased), leading to a Cnet of −7.6 $\mathrm{Tg\,C\,yr^{-1}}$ (Fig. 4f). The net effect on GHWP was a larger increase from its historical value (to 100 $\mathrm{Tg\,CO_2\,yr^{-1}}$) than for Warming + LAI (Fig. 4g), but still smaller than for warming alone.

The combination of drying and increased LAI (Warming + Drying + LAI; red bars) also acted in opposition to warming alone. This simulation predicted greater drying than Warming + Drying: end-of-century values of $\mathrm{Asat_{JJA}}$ and $\mathrm{WTD_{JJA}}$ were 0.27 and 23 cm, or 42 % less and 36 % greater than their historical values, respectively (Fig. 4b and c). Drier soils and greater photosynthesizing area led to the largest increases in NPP and Rh of all simulations, with values of 250 and 220 $\mathrm{Tg\,C\,yr^{-1}}$ (Fig. 4c and d). In contrast, drier soils led to the smallest increase in end-of-century $\mathrm{CH_4}$ of all simulations, to 6.2 $\mathrm{Tg\,CH_4\,yr^{-1}}$ (86 % above historical, Fig. 4e). Greater carbon uptake (Cnet of −23 $\mathrm{Tg\,C\,yr^{-1}}$, Fig. 4f) and lower $\mathrm{CH_4}$ emissions led to the smallest increase in end-of-century GHWP of all simulations, of 29 $\mathrm{Tg\,CO_2\,yr^{-1}}$ (approximately 2.6 times its historical value; Fig. 4g).

Thus, the combination of drier soils and greater photosynthesizing area only partially offset the effects of warming on $\mathrm{CH_4}$ and GHWP, but surpassed the effects of warming on carbon uptake (Cnet). For these fluxes, warming increased the flux of carbon to the atmosphere, while drying (both LAI- and climate-driven) reduced the flux to the atmosphere. While increased LAI (without drying), had little influence over CH_4, it played a major role in reducing the net flux to the atmosphere for Cnet and GHWP. There were two exceptions to these patterns. In the south, the drying due to both climate and LAI caused some grid cells to experience water limitation, which slowed the increase of NPP and carbon uptake (Fig. 4c and f). In contrast, in the north, wetlands were more likely to be temperature-limited than water-limited; thus, CH_4 fluxes there responded primarily to warming, and showed a small but positive response to increased LAI with drying (Fig. 4e and Table 5).

For CH_4, the opposing influences of warming and drying are consistent with the negative climate-wetland CH_4 feedback explored by Ringeval et al. (2011) and Koven et al. (2011). To estimate its size, Ringeval et al. and Koven et al. compared simulations with fixed wetland extent (analogous to our Warming + LAI simulations, because they used a DGVM) to simulations with varying wetland extent (analogous to our Warming + Drying + LAI simulations). Koven et al. found that drying reduced the 21st century increases in CH_4 yielded by warming by 60–80 % over the Arctic. Based on the difference between the predictions of our Warming + LAI (green) and Warming + Drying + LAI (red) simulations, we estimate the size of this effect over the WSL to be $-1.8\,\mathrm{Tg\,CH_4\,yr^{-1}}$, or only 38 % of the size of the effect of future warming (Warming + LAI minus Historical).

3.3 Microbial acclimatization and population shifts

Acclimatization and population shifts proved to be potentially more important than climate and LAI as a factor in our results. Figure 5 shows the predicted CH_4 and GHWP emissions for the same set of simulations as Fig. 4, for the three cases of soil microbial response (Cnet was relatively insensitive to soil microbe response and is not plotted). Relative to the NoAcc + NoShift simulations (Fig. 5a and b), applying acclimatization but not population shifts (Acc + NoShift; Fig. 5c and d) dramatically reduced the end-of-century CH_4 emissions over the WSL to 3.57 Tg CH_4 yr^{-1} (only 6 % greater than historical emissions), and turned the domain into a net GHWP sink of −28 Tg CO_2 yr^{-1}. This is consistent with Koven et al. (2011), who found that acclimatization eliminated 50–75 % of the increases predicted by simulations that did not account for acclimatization (note that the curves in their Fig. 4 for fixed and varying Tmean were mis-labeled; Koven and Ringeval, personal communication, 2013). These changes were most pronounced in the south, where warming in the presence of acclimatization led to only a meager increase in CH_4 emissions, for which climate- and LAI-induced drying more than compensated, leading to future CH_4 emissions (1.97 Tg C yr^{-1}) that were 15 % lower than historical. In the north, acclimatization had only a slight effect on CH_4 and GHWP.

In contrast, adding population shifts to the acclimatization simulations (Acc + Shift; Fig. 5e and f) yielded larger increases in CH_4 emissions over the WSL (7.36 Tg CH_4 yr^{-1}, or 119 % above historical values) than the NoAcc + NoShift case (6.25 Tg CH_4 yr^{-1}, or 85 % above historical values). Similarly, GHWP emissions rose to 52 Tg CO_2 yr^{-1}, compared to 29 Tg CO_2 yr^{-1} for the NoAcc + NoShift case. However, unlike the NoAcc + NoShift case, in which approximately 2/3 of future CH_4 emissions were generated in the south, 73 % of future CH_4 emissions were generated in the north (where emissions increased by a factor of five over historical values) for the Acc + Shift case. The reason for this is that we modeled population shifts as a complete replacement of the northern microbial species abundances (and their response to temperature) with those of the southern microbial communities. Thus, in the south, there was no change in the CH_4 parameter set; acclimatization worked as it did in the acclimatization/no population shift simulations. In the north, the introduction of the greater southern temperature sensitivity allowed for larger emissions during the growing season, despite the elevated Tmean. Population shifts also amplified the north's small but positive response to increased LAI with drying.

For the WSL as a whole, the range of CH_4 emissions bracketed by the median results for the presence or absence of acclimatization and population shifts was nearly as large (3.8 Tg CH_4 yr^{-1}) as the effect of warming alone in the NoAcc + NoShift simulations (which added 4.2 Tg CH_4 yr^{-1}), and more than twice the size of the effect of the climate-wetland CH_4 feedback for the NoAcc + NoShift case (1.8 Tg CH_4 yr^{-1}). For the north in particular, the range of values bracketed by the soil microbial response cases (3.8 Tg CH_4 yr^{-1}) was almost four times the size of the effect of warming alone in the NoAcc + NoShift case (1.0 Tg CH_4 yr^{-1}). It should be noted, however, that the primary mechanism by which population shifts and acclimatization acted was changing the temperature sensitivity, so that their effects constitute a modulation of the warming effect.

Acclimatization (with or without population shifts) reduced the size of the climate-wetland CH_4 feedback to −1.1 Tg CH_4 yr^{-1}. At the same time, the warming (Warming + LAI minus Historical) effect decreased to 1.3 Tg CH_4 yr^{-1} under acclimatization and increased to 5.1 Tg CH_4 yr^{-1} under acclimatization plus population shifts. Thus, the various soil microbial responses caused the strength of the climate-wetland CH_4 feedback to be between 22 and 85 % of the warming effect, the upper bound of which is more consistent with the estimate of Koven et al. (2011) for the entire Arctic (60–80 % of the warming effect).

3.4 Effects on seasonal cycle

Acclimatization and population shifts not only affected total annual CH_4 emissions, but also changed the shape of the seasonal cycle of emissions in the northern half of the WSL. Monthly spatial average methane emissions and hydrologic terms over the period 2071–2100 are plotted in Fig. 6, for the southern and northern halves of the WSL. During snowmelt (Fig. 6c and d), the upper soil layers begin to thaw (Fig. 6e and f). Without acclimatization or population shifts, the north's lower temperature sensitivity (Q10) leads to lower CH_4 emissions throughout the growing season than in the south (solid black lines in Fig. 6a and b), despite the north's wetter and more anoxic conditions (evidenced by larger saturated fraction and higher water table, Fig. 6g and h and

Fig. 6i and j, respectively) and the presence of labile carbon substrate (to which NPP is a contributor, Fig. 6k and l). By raising Tmean, acclimatization reduces the temperature response in both the south and the north (dashed blue lines, Fig. 6a and b), but in the north, the difference is relatively small due to the lower Q10 there.

Population shifts (red dot-dashed lines, Fig. 6a and b) had little effect in the south, but made a large difference in the north, where the increase in Q10 allowed microbes to take advantage of both the warming temperatures and the wetter conditions, leading to larger emissions than were achieved in the south even without acclimatization. In addition, population shifts disproportionately increased emissions (by a factor of 3.8 to 4.2, relative to no shifts) in the first half of the growing season, during and immediately after snowmelt (Fig. 6b), when conditions are wettest. Later in the growing season, increases in emissions are smaller (only a factor of 1.5 to 2 relative to no dispersal) due to drier soils and their accompanying methanotrophy. The net result is to shift the peak emissions forward in time. The implications of increased methanogenic activity during and immediately after snowmelt are discussed further in Sect. 4.

4 Discussion

Our results suggest that the potential response of soil microbial communities to changes in climate and vegetation is as important as climate change itself to predicting future high-latitude wetland methane emissions. More importantly, the soil microbial response has the potential to shift emissions to the northern portion of the WSL, where uncertainty about the potentially large amount of labile carbon that might be liberated by permafrost thaw (not explicitly considered in this study) is also a concern (Koven et al., 2011; Schaefer et al., 2011; Zimov et al., 2006). In particular, Schaefer et al. predicted a median cumulative flux to the atmosphere from present-day permafrost soils of about 80 Gt C between 2020 and 2100, and estimated it could lead to an increase in atmospheric carbon of 25 % over current levels. Whether this additional carbon will be respired as CO_2 or CH_4 depends crucially on the degrees of microbial acclimatization and population shifts that will occur. Futhermore, our findings indicate that population shifts not only could increase CH_4 emissions in the permafrost zone, but also could increase uncertainty in those emissions via increased sensitivity to temperature.

The increased temperature sensitivity in the northern half of the domain brought about by population shifts, and the disproportionate increase in microbial activity during snowmelt that results, may result in a larger increase in CH_4 emissions than we have predicted. Studies have found that the dissolved organic carbon (DOC) in boreal and Arctic streams is most labile (easily consumable by microbes) during the snowmelt freshet, followed by a decline over the course of the summer (Mann et al., 2012; Holmes et al., 2008), suggesting that the onset of snowmelt and soil thaw liberates highly labile carbon from the soil. Observations suggest that, during the lower flow conditions after snowmelt, wetland microbes preferentially consume labile DOC faster than it is input by local plants (Olefeldt and Roulet, 2012), so that lability declines with distance downstream and with residence time in the wetland. Our modeling framework does not explicitly represent the lability of carbon or its preferential consumption by microbes, and therefore likely underestimates the lability of the carbon available during snowmelt. Given that the labile DOC consumed by wetland microbes would otherwise be exported to the relatively oxic stream network, where it could be metabolized and outgassed as CO_2 (Wallin et al., 2013), the degree to which soil microbes influence the export of labile DOC to streams is an important factor to constrain.

While our results corroborated both the climate-wetland CH_4 feedback and the acclimatization estimated by Ringeval et al. (2011) and Koven et al. (2011), our estimate of the climate-wetland CH_4 feedback effect size was smaller than theirs (22–38 % of the size of the warming effect, vs. 60–80 %), and our estimate of acclimatization was larger (85 % of the size of the warming effect, vs. 50 %). One reason for this may be that our acclimatization approach set Tmean equal to the 10 yr moving average of soil temperature, while Ringeval et al. and Koven et al. used a relaxation approach with a 365 day time constant, in which the previous winter's soil temperatures might have a larger influence than in our approach. Another potential reason for the discrepancy might be their neglect of emissions from wetlands where the water table depth is deeper than 5 cm, which could affect sensitivities to climate change (Bohn and Lettenmaier, 2010). Another reason may be that Ringeval et al. and Koven et al. applied a single methane emissions parameter set globally, which may have yielded a positive bias in historical methane emissions over the northern WSL (Bohn et al., 2013b). The higher historical baseline emissions in the north might have reduced the size of the warming effect in their simulations. Their more productive northern emissions (and their use of a single parameter set globally) suggest that their end-of-century results might correspond more closely to our Acc + Shift simulation than our Acc + NoShift simulation. Conversely, the historical/current net value of the climate-wetland CH_4 feedback over the high latitudes may be more negative than estimated by Ringeval et al.

Modeling population shifts as an expansion of the range over which we apply the southern CH_4 parameter set may be an oversimplification in several ways:

1. The new microbial communities in the north will not necessarily be identical to those currently in the south, due to different local conditions (e.g., soil pH, subsurface flow, etc.). It is not clear whether our assumptions might effectively be an upper bound, because we do not know if new combinations of species (especially different abundances of methanogens and methanotrophs) will produce larger or smaller net CH_4 emissions. Pickels et al. (2012) noted that different fungi species disperse at different rates, and that community dominance often depends on the order of species arrival. In addition, some microbes are symbiotic with plant hosts, which will also experience varying rates of dispersal. How microbe and plant abundances might evolve through time and space, and how that would affect carbon fluxes, is poorly known (e.g., Conant et al., 2011; Olsrud et al., 2004).

2. We modeled population shifts as a complete replacement of species abundances across the entire domain; in reality population shifts might be limited in geographic extent by climate. Thus, we may have produced something close to an upper bound on the changes in the north.

3. We did not change the CH_4 parameters used in the south. It is possible that southern mires might also experience changes in species assemblages, perhaps evolving to resemble temperate communities, which are potentially more productive (e.g., Yavitt et al., 2012). Thus, this is a lower bound on the changes in the south.

4. We did not vary plant-aided transport parameters spatially and thus could not model any potential changes in geographic distribution of vascular plants that have aerenchyma. Previous studies (Riley et al., 2011; Berrittella and van Huissteden, 2011) found that CH_4 emissions were sensitive to plant-aided transport, and in particular, Berrittella and van Huissteden (2011) found that differences in the distributions of plants with aerenchyma had a strong influence on Ice Age CH_4 emissions. However, any influence that plant-aided transport might have on the current distribution of CH_4 emissions would presumably shift northward along with the plants themselves, contributing to the increase in emissions in the northern half of the domain.

5. We did not consider other spatially-varying factors like nutrient (N and P) concentrations, pH, redox state, or the oxidation of methane in the water column in inundated wetlands (for more details, see Bohn et al., 2013b). It is not yet clear how these factors will respond to future climate change.

Our results reinforce the findings of Bohn et al. (2013b), that spatial variation in soil microbial behavior (reflected in CH_4 emissions parameters) exerts an important control on large-scale wetland carbon fluxes. No other studies have examined microbial population shifts, in part because few large-scale models have applied spatially-varying parameters. This, in turn, is partly due to a lack of sufficient long-term in situ observations to support spatially-varying parameters. However, with the advent of intensive data sets such as Glagolev et al. (2011) and Peregon et al. (2009) in the WSL and Levy et al. (2012) in the UK, it should become possible to find linkages between vegetation and CH_4 parameters that enable parameter transfer over regions where few in situ observations have been made.

5 Conclusions

We used the Variable Infiltration Capacity (VIC) land surface model (Liang et al., 1994), linked to the wetland methane emissions model of Walter and Heimann (2000), forced off-line with outputs of CMIP5 projections (Taylor, et al., 2012) for the RCP 4.5 pathway, to simulate changes in the surface hydrology and methane emissions of the wetlands of the West Siberian Lowland. We examined the effects on end-of-century CH_4 emissions of changes in climate and LAI, and the possible responses of soil microbes to these changes. We conclude that:

- By the end of this century, CH_4 emissions from the WSL will rise to 3.6–7.3 Tg CH_4 yr^{-1}, an increase of 6–119 % over their historical values. Carbon uptake by the region's wetlands will increase to 23 Tg C yr^{-1} from a historical level of 14 Tg C yr^{-1}. The net greenhouse warming potential of the region's wetlands will range between –22 to 51 Tg CO_2 yr^{-1}.
- The potential response of soil microbes to future changes in climate and vegetation is as important as climate change in determining future greenhouse gas emissions from high-latitude wetlands. Acclimatization almost completely offset the increases in CH_4 emissions that arose from changes in climate and LAI, while population shifts led to a near doubling of the region's emissions. Crucially, while ignoring acclimatization and population shifts focused the majority of emissions in the southern half of the domain, acclimatization plus population shifts concentrated 73 % of future emissions in the northern half of the domain, where the possible release of carbon with permafrost thaw is a concern.
- Population shifts increased microbial activity during and immediately following snowmelt, when highly labile carbon is thought to be first released from the soil.

This may imply larger CH_4 emissions than we have predicted, and a possible reduction of the labile carbon exported to Arctic streams.

Our work indicates the importance of better constraining the responses of soil microbial communities to changes in climate and vegetation as they are critical determinants of the region's future methane emissions.

Acknowledgements. This work was funded by grants NNX08AH97G and NNX09AK57G from NASA to the University of Washington. Advanced computational, storage, and networking infrastructure was provided in part by the University of Washington's Hyak supercomputer system, supported in part by the University of Washington eScience Institute.

References

Adam, J. C. and Lettenmaier, D. P.: Adjustment of global gridded precipitation for systematic bias, J. Geophys. Res., 108, 1–14, doi:10.1029/2002JD002499, 2003.

Adam, J. C. and Lettenmaier, D. P.: Application of new precipitation and reconstructed streamflow products to streamflow trend and attribution in northern Eurasia, J. Climate, 21, 1807–1828, doi:10.1175/2007JCLI1535.1, 2008.

Adam, J. C., Clark, E. A., Lettenmaier, D. P., and Wood, E. F.: Correction of global precipitation products for orographic effects, J. Climate, 19, 15–38, doi:10.1175/JCLI3604.1, 2006.

Allison, S. D., Wallenstein, M. D., and Bradford, M. A.: Soil-carbon response to warming dependent on microbial physiology, Nat. Geosci., 3, 336–340, doi:10.1038/NGEO846, 2010.

Alo, C. A. and Wang, G.: Potential future changes of the terrestrial ecosystem based on climate projections by eight general circulation models, J. Geophys. Res.-Biogeo., 113, G01004, doi:10.1029/2007JG000528, 2008a.

Alo, C. A. and Wang, G.: Hydrological impact of the potential future vegetation response to climate changes projected by 8 GCMs, J. Geophys. Res.-Biogeo., 113, G03011, doi:10.1029/2007JG000598, 2008b.

Berrittella, C. and van Huissteden, J.: Uncertainties in modelling CH_4 emissions from northern wetlands in glacial climates: the role of vegetation parameters, Clim. Past, 7, 1075–1087, doi:10.5194/cp-7-1075-2011, 2011.

Bohn, T. J., Lettenmaier, D. P., Sathulur, K., Bowling, L. C., Podest, E., McDonald, K. C., and Friborg, T.: Methane emissions from western Siberian wetlands: heterogeneity and sensitivity to climate change, Environ. Res. Lett., 2, 045015, doi:10.1088/1748-9326/2/4/045015, 2007.

Bohn, T. J. and Lettenmaier, D. P.: Systematic biases in large-scale estimates of wetland methane emissions arising from water table formulations, Geophys. Res. Lett., 37, L22401, doi:10.1029/2010GL045450, 2010.

Bohn, T. J., Livneh, B., Oyler, J. W., Running, S. W., Nijssen, B., and Lettenmaier, D. P.: Global evaluation of MTCLIM and related algorithms for forcing of ecological and hydrological models, Agr. Forest Meteorol., 176, 38–49, doi:10.1016/j.agrformet.2013.03.003, 2013a.

Bohn, T. J., Podest, E., Schroeder, R., Pinto, N., McDonald, K. C., Glagolev, M., Filippov, I., Maksyutov, S., Heimann, M., Chen, X., and Lettenmaier, D. P.: Modeling the large-scale effects of surface moisture heterogeneity on wetland carbon fluxes in the West Siberian Lowland, Biogeosciences, 10, 6559–6576, doi:10.5194/bg-10-6559-2013, 2013b.

Bowling, L. C. and Lettenmaier, D. P.: Modeling the effects of lakes and wetlands on the water balance of Arctic environments, J. Hydrometeorol., 11, 276–295, doi:10.1175/2009JHM1084.1, 2010.

Brodzik, M. J. and Knowles, K. W.: EASE-Grid: a versatile set of equal-area projections and grids, in: Discrete Global Grids, edited by: Goodchild, M., available at: http://www.ncgia.ucsb.edu/globalgrids-book/ease_grid/ (last access: 4 April 2013), National Center for Geographic Information and Analysis, Santa Barbara, California USA, 2002.

Cherkauer, K. A. and Lettenmaier, D. P.: Hydrologic effects of frozen soils in the upper Mississippi River Basin, J. Geophys. Res.-Atmos., 104, 19599–19610, doi:10.1029/1999JD900337, 1999.

Christensen, T. R., Ekberg, A., Strom, L., Mastepanov, M., Panikov, N., Oquist, M., Svensson, B. H., Martikainen, P. J., and Oskarsson, H.: Factors controlling large scale variations in methane emissions from wetlands, Geophys. Res. Lett., 30, 1414, doi:10.1029/2002GL016848, 2003.

Christensen, T. R., Johansson, R. T., Akerman, H. J., Mastepanov, M., Malmer, N., Friborg, T., Crill, P., and Svensson, B. H.: Thawing sub-arctic permafrost: effects on vegetation and methane emissions, Geophys. Res. Lett., 31, L04501, doi:10.1029/2003GL018680, 2004.

Conant, R. T., Ryan, M. G., Agren, G. I., Birge, H. E., Davison, E. A., Eliasson, P. E., Evans, S. E., Frey, S. D., Giardina, C. P., Hopkins, F. M., Hyvonen, R., Kirschbaum, M. U. F., Lavallee, J. M., Leifeld, J., Parton, W. J., Steinweg, J. M., Wallenstein, M. D., Wetterstedt, J. A. M., and Bradford, M. A.: Temperature and soil organic matter decomposition rates – synthesis of current knowledge and a way forward, Glob. Change Biol., 17, 3392–3404, doi:10.1111/j.1365-2486.2011.02496.x, 2011.

Contosta, A. R., Frey, S. D., Ollinger, S. V., and Cooper, A. B.: Soil respiration does not acclimatize to warmer temperatures when modeled over seasonal timescales, Biogeochemistry, 112, 555–570, doi:10.1007/s10533-012-9748-6, 2013.

DeLeon-Rodriguez, N., Lathem, T. L., Rodriguez-R, L. M., Barazesh, J. M., Anderson, B. E., Beyersdorf, A. J., Ziemba, L. D., Bergin, M., Nenes, A., and Konstantinidis, K. T.: Microbiome of the upper troposphere: species composition and prevalence, effects of tropical storms, and atmospheric implications, P. Natl. Acad. Sci. USA, 110, 2575–2580, doi:10.1073/pnas.1212089110, 2013.

Diffenbaugh, N. S. and Giorgi, F.: Climate change hotspots in the CMIP5 global climate model ensemble, Climatic Change, 114, 813–822, doi:10.1007/s10584-012-0570-x, 2012.

Dise, N. B., Gorham, E., and Verry, S.: Environmental factors controlling methane emissions from peatlands in Northern Minnesota, J. Geophys. Res.-Atmos., 98, 10583–10594, doi:10.1029/93JD00160, 1993.

Dumbrell, A. J., Nelson, M., Helgason, T., Dytham, C., and Fitter, A. H.: Relative roles of niche and neutral processes in structuring a soil microbial community, ISME J., 4, 337–345, doi:10.1038/ismej.2009.122, 2010.

Eliseev, A. V., Mokhov, I. I., Arzhanov, M. M., Demchenko, P. F., and Denisov, S. N.: Interaction of the methane cycle and processes in wetland ecosystems in a climate model of intermediate complexity, Iz. An. SSSR. Fiz. Atm.+, 44, 139–152, doi:10.1134/S0001433808020011, 2008.

Frey, K. E. and Smith, L. C.: Amplified carbon release from West Siberian peatlands by 2100, Geophys. Res. Lett., 32, L09401, doi:10.1029/2004GL022025, 2005.

Finlay, B. J. and Clarke, K. J.: Ubiquitous dispersal of microbial species, Nature, 400, 828–828, doi:10.1038/23616, 1999.

Gedney, N., Cox, P. M., and Huntingford, C.: Climate feedback from wetland methane emissions, Geophys. Res. Lett., 31, L20503, doi:10.1029/2004GL020919, 2004.

Glagolev, M., Kleptsova, I., Filippov, I., Maksyutov, S., and Machida, T.: Regional methane emission from West Siberia mire landscapes, Environ. Res. Lett., 6, 045214, doi:10.1088/1748-9326/6/4/045214, 2011.

Graham, D. E., Wallenstein, M. D., Vishnivetskaya, T. A., Waldrop, M. P., Phelps, T. J., Pfiffner, S. M., Onstott, T. C., Whyte, L. G., Rivkina, E. M., Gilichinsky, D. A., Elias, D. A., Mackelprang, R., VerBerkmoes, N. C., Hettich, R. L., Wagner, D., Wullschleger, S. D., and Jansson, J. K.: Microbes in thawing permafrost: the unknown variable in the climate change equation, ISME J., 6, 709–712, doi:10.1038/ismej.2011.163, 2012.

Hamlet, A. F. and Lettenmaier, D. P.: Effects of climate change on hydrology and water resources in the Columbia River Basin, J. Am. Water Resour. As., 35, 1597–1623, doi:10.1111/j.1752-1688.1999.tb04240.x, 1999.

Holmes, R. M., McClelland, J. W., Peterson, B. J., Tank, S. E., Bulygina, E., Eglinton, T. I., Gordeev, V. V., Gurtovaya, T. Y., Raymond, P. A., Repeta, D. J., Staples, R., Striegl, R. G., Zhulidov, A. V., and Zimov, S. A.: Seasonal and annual fluxes of nutrients and organic matter from large rivers to the Arctic Ocean and surrounding seas, Estuar. Coast., 35, 369–382, doi:10.1007/s12237-011-9386-6, 2008.

Intergovernmental Panel on Climate Change (IPCC): Climate Change 2007: The Physical Science Basis. Contribution of Working Group I to the Fourth Assessment Report of the Intergovernmental Panel on Climate Change, edited by: Solomon, S., Qin, D., Manning, N., Chen, Z., Marquis, M., Averyt, K. B., Tignor, M., and Miller, H. L., Cambridge University Press, Cambridge, 996 pp., 2007.

Jiang, Y. Y., Zhuang, Q. L., Schaphoff, S., Sitch, S., Sokolov, A., Kicklighter, D., and Melillo, J.: Uncertainty analysis of vegetation distribution in the northern high latitudes during the 21st century with a dynamic vegetation model, Ecol. Evol., 2, 593–614, doi:10.1002/ece3.85, 2012.

Kaplan, J. O. and New, M.: Arctic climate change with a 2 °C global warming: timing, climate patterns and vegetation change, Climatic Change, 79, 213–241, doi:10.1007/s10584-006-9113-7, 2006.

Koven, C. D., Ringeval, B., Friedlingstein, P., Ciais, P., Cadule, P., Khvorostyanov, D., Krinner, G., and Tarnocai, C.: Permafrost carbon-climate feedbacks accelerate global warming, P. Natl. Acad. Sci. USA, 108, 14769–14774, doi:10.1073/pnas.1103910108, 2011.

Kremenetski, K. V., Velichko, A. A., Borisova, O. K., MacDonald, G. M., Smith, L. C., Frey, K. E., and Orlova, L. A.: Peatlands of the Western Siberian lowlands: current knowledge on zonation, carbon content and late Quaternary history, Quaternary Sci. Rev., 22, 703–723, doi:10.1016/S0277-3791(02)00196-8, 2003.

Lehner, B. and Döll, P.: Development and validation of a global database of lakes, reservoirs, and wetlands, J. Hydrol., 296, 1–22, doi:10.1016/j.jhydrol.2004.03.028, 2004.

Levy, P. E., Burden, A., Cooper, M. D. A., Dinsmore, K. J., Drewer, J., Evans, C., Fowler, D., Gaiawyn, J., Gray, A., Jones, S. K., Jones, T., McNamara, N. P., Mills, R., Ostle, N., Sheppard, L. J., Skiba, U., Sowerby, A., Ward, S. E., and Zielinski, P.: Methane emissions from soils: synthesis and analysis of a large UK data set, Glob. Change Biol., 18, 1657–1669, doi:10.1111/j.1365-2486.2011.02616.x, 2012.

Liang, X., Lettenmaier, D. P., Wood, E. F., and Burges, S. J.: A simple hydrologically based model of land-surface water and energy fluxes for general-circulation models, J. Geophys. Res., 99, 14415–14428, doi:10.1029/94JD00483, 1994.

Limpens, J., Berendse, F., Blodau, C., Canadell, J. G., Freeman, C., Holden, J., Roulet, N., Rydin, H., and Schaepman-Strub, G.: Peatlands and the carbon cycle: from local processes to global implications – a synthesis, Biogeosciences, 5, 1475–1491, doi:10.5194/bg-5-1475-2008, 2008.

Lupascu, M., Wadham, J. L., Hornibrook, E. R. C., and Pancost, R. D.: Temperature sensitivity of methane production in the permafrost active layer at Stodalen, Sweden: a comparison with non-permafrost northern wetlands, Arct. Antarct. Alp. Res., 44, 469–482, doi:10.1657/1938-4246-44.4.469, 2012.

Mann, P. J., Davydova, A., Zimov, N., Spencer, R. G. M., Davydov, S., Bulygina, E., Zimov, S., and Holmes, R. M.: Controls on the composition and lability of dissolved organic matter in Siberia's Kolyma River Basin, J. Geophys. Res.-Biogeo., 117, G01028, doi:10.1029/2011JG001798, 2012.

Melton, J. R., Wania, R., Hodson, E. L., Poulter, B., Ringeval, B., Spahni, R., Bohn, T., Avis, C. A., Beerling, D. J., Chen, G., Eliseev, A. V., Denisov, S. N., Hopcroft, P. O., Lettenmaier, D. P., Riley, W. J., Singarayer, J. S., Subin, Z. M., Tian, H., Zürcher, S., Brovkin, V., van Bodegom, P. M., Kleinen, T., Yu, Z. C., and Kaplan, J. O.: Present state of global wetland extent and wetland methane modelling: conclusions from a model inter-comparison project (WETCHIMP), Biogeosciences, 10, 753–788, doi:10.5194/bg-10-753-2013, 2013.

Mitchell, T. D. and Jones, P. D.: An improved method of constructing a database of monthly climate observations and associated high-resolution grids, Int. J. Climatol., 25, 693–712, doi:10.1002/joc.1181, 2005.

Moss, R. H., Edmonds, J. A., Hibbard, K. A., Manning, M. R., Rose, S. K., van Vuuren, D. P., Carter, T. R., Emori, S., Kainuma, M., Kram, T., Meehl, G. A., Mitchell, J. F. B., Nakicenovic, N., Riahi, K., Smith, S. J., Stouffer, R. J., Thomson, A. M., Weyant, J. P., and Wilbanks, T. J.: The next generation of scenarios for climate change research and assessment, Nature, 463, 747–756, doi:10.1038/nature08823, 2010.

Myneni, R. B., Hoffman, S., Knyazikhin, Y., Privette, J. L., Glassy, J., Tian, Y., Wang, Y., Song, X., Zhang, Y., Smith, G. R., Lotsch, A., Friedl, M., Morisette, J. T., Votava, P., Nemani, R. R., and Running, S. W.: Global products of vegetation leaf area and fraction absorbed PAR from year one of MODIS data, Remote Sens. Environ., 83, 214–231, doi:10.1016/S0034-4257(02)00074-3, 2002.

Olefeldt, D. and N. Roulet: Effects of permafrost and hydrology on the composition and transport of dissolved organic carbon in a subarctic peatland complex, J. Geophys. Res.-Biogeo., 117, G01005, doi:10.1029/2011JG001819, 2012.

Olefeldt, D., Turetsky, M. R., Crill, P. M., and McGuire, A. D.: Environmental and physical controls on northern terrestrial methane emissions acros permafrost zones, Glob. Change Biol., 19, 589–603, doi:10.1111/gcb.12071, 2013.

Olsrud, M., Melillo, J. M., Christensen, T. R., Michelsen, A., Wallander, H., and Olsson, P. A.: Response of ericoid mycorrhizal colonization and functioning to global change factors, New Phytol., 162, 459–469, doi:10.1111/j.1469-8137.2004.01049.x, 2004.

Panofsky, H. A. and Brier, G. W.: Some Applications of Statistics to Meteorology, The Pennsylvania State University, University Park, 224 pp., 1968.

Peregon, A., Maksyutov, S., and Yamagata, Y.: An image-based inventory of the spatial structure of West Siberian wetlands, Environ. Res. Lett., 4, 045014, doi:10.1088/1748-9326/4/4/045014, 2009.

Pickles, B. J., Egger, K. N., Massicotte, H. B., and Green, D. S.: Ectomycorrhizas and climate change, Fungal Ecol., 5, 73–84, doi:10.1016/j.funeco.2011.08.009, 2012.

Raymond, P. A., McClelland, J. W., Holmes, R. M., Zhulidov, A. V., Mull, K., Peterson, B. J., Striegl, R. G., Aiken, G. R., and Gurtovaya, T. Y.: Flux and age of dissolved organic carbon exported to the Arctic Ocean: a carbon isotopic study of the five largest arctic rivers, Global Biogeochem. Cy., 21, GB4011, doi:10.1029/2007GB002934, 2007.

Riley, W. J., Subin, Z. M., Lawrence, D. M., Swenson, S. C., Torn, M. S., Meng, L., Mahowald, N. M., and Hess, P.: Barriers to predicting changes in global terrestrial methane fluxes: analyses using CLM4Me, a methane biogeochemistry model integrated in CESM, Biogeosciences, 8, 1925–1953, doi:10.5194/bg-8-1925-2011, 2011.

Ringeval, B., de Noblet-Ducoudré, N., Ciais, P., Bousquet, P., Prigent, C., Papa, F., and Rossow, W. B.: An attempt to quantify the impact of changes in wetland extent on methane emissions on the seasonal and interannual time scales, Global Biogeochem. Cy., 24, GB2003, doi:10.1029/2008GB003354, 2010.

Ringeval, B., Friedlingstein, P., Koven, C., Ciais, P., de Noblet-Ducoudré, N., Decharme, B., and Cadule, P.: Climate-CH_4 feedback from wetlands and its interaction with the climate-CO_2 feedback, Biogeosciences, 8, 2137–2157, doi:10.5194/bg-8-2137-2011, 2011.

Saarnio, S., Alm, J., Silvola, J., Lohila, A., Nykänen, H., and Martikainen, P. J.: Seasonal variation in CH_4 emissions and production and oxidation potentials at microsites of an oligotrophic pine fen, Oecologia, 110, 414–422, 1997.

Schaefer, K., Zhang, T., Bruhwiler, L., and Barrett, A. P.: Amount and timing of permafrost carbon release in response to climate warming, Tellus B, 63, 165–180, doi:10.1111/j.1600-0889.2011.00527.x, 2011.

Serreze, M. C., Walsh, J. E., Chapin, F. S., Osterkamp, T., Dyurgerov, M., Romanovsky, V., Oechel, W. C., Morison, J., Zhang, T., and Barry, R. G.: Observational evidence of recent change in the northern high-latitude environment, Climatic Change, 46, 159–207, doi:10.1023/A:1005504031923, 2000.

Sheffield, J., Goteti, G., and Wood, E. F.: Development of a 50-year high-resolution global dataset of meteorological forcings for land surface modeling, J. Climate, 19, 3088–3111, doi:10.1175/JCLI3790.1, 2006.

Sheng, Y. W., Smith, L. C., MacDonald, G. M., Kremenetski, K. V., Frey, K. E., Velichko, A. A., Lee, M., Beilman, D. W., and Dubinin, P.: A high-resolution GIS-based inventory of the west Siberian peat carbon pool, Global Biogeochem. Cy., 18, GB3004, doi:10.1029/2003GB002190, 2004.

Sitch, S., Huntingford, C., Gedney, N., Levy, P. E., Lomas, M., Piao, S. L., Betts, R., Ciais, P., Cox, P., Friedlingstein, P., Jones, C. D., Prentice, I. C., and Woodward, F. I.: Evaluation of the terrestrial carbon cycle, future plant geography and climate-carbon cycle feedbacks using five Dynamic Global Vegetation Models (DGVMs), Glob. Change Biol., 14, 2015–2039, doi:10.1111/j.1365-2486.2008.01626.x, 2008.

Taylor, K. E., Stouffer, R. J., and Meehl, G. A.: An overview of CMIP5 and the experiment design, B. Am. Meteorol. Soc., 93, 485–498, doi:10.1175/BAMS-D-11-00094.1, 2012.

Wallin, M. B., Grabs, T., Buffam, I., Laudon, H., Ågren, A., Öquist, M. G., and Bishop, K.: Evasion of CO_2 from streams – the dominant component of the carbon export through the aquatic conduit in a boreal landscape, Glob. Change Biol., 19, 785–797, doi:10.1111/gcb.12083, 2013.

Walter, B. P. and Heimann, M.: A process-based, climate-sensitive model to derive methane emissions from natural wetlands: application to five wetland sites, sensitivity to model parameters, and climate, Global Biogeochem. Cy., 14, 745–765, doi:10.1029/1999GB001204, 2000.

Walter, K. M., Zimov, S. A., Chanton, J. P., Verbyla, D., and Chapin III, F. S.: Methane bubbling from Siberian thaw lakes as a positive feedback to climate warming, Nature, 443, 71–75, doi:10.1038/nature05040, 2006.

Wania, R., Ross, I., and Prentice, I. C.: Integrating peatlands and ermafrost into a dynamic global vegetation model: 2. Evaluation and sensitivity of vegetation and carbon cycle processes, Global Biogeochem. Cy., 23, GB3015, doi:10.1029/2008GB003413, 2009.

Willmott, C. J. and Matsuura, K.: Terrestrial air temperature and precipitation: monthly and annual time series (1950–1999) (version 1.02), Center for Climate Research., University of Delaware, Newark, DE, available at: http://climate.geog.udel.edu/~climate/html_pages/archive.html (last access: 1 January, 2012), 2001.

Yavitt, J. B., Yashiro, E., Cadillo-Quiroz, H., and Zinder, S. H.: Methanogen diversity and community composition in peatlands of the central to northern Appalachian Mountain region, North America, Biogeochemistry, 109, 117–131, doi:10.1007/s10533-011-9644-5, 2012.

Zimov, S. A., Davydov, S. P., Zimova, G. M., Davydova, A. I., Schuur, E. A. G., Dutta, K, and Chapin, F. S.: Permafrost carbon: stock and decomposability of a globally significant carbon pool, Geophys. Res. Lett., 33, L20502, doi:10.1029/2006GL027484, 2006.

Table 1. Parameter values of the wetland methane emissions model of Walter and Heimann (2000). The values reported are the medians from Bohn et al. (2013b).

Parameter	Units	Value	
		South	North
$r0$ [1]	$(\mathrm{g\,C\,m^{-2}\,d^{-1}})^{-1}$	0.019	0.020
Xvmax	$\mathrm{\mu mol\,L^{-1}\,h^{-1}}$	0.24	0.14
Rkm	$\mathrm{\mu mol\,L^{-1}}$	16.1	11.0
rq10	unitless	10.7	3.4
oxq10	unitless	2.1	4.9

[1] As documented in Bohn et al. (2013b), we modified the NPP dependence of the methane emissions model, resulting in the originally unitless $r0$ parameter taking on units of $[(\mathrm{g\,C\,m^{-2}\,d^{-1}})^{-1}]$.

Table 2. CMIP5 model outputs used in this study[1].

Model	Dynamic vegetation	Model	Dynamic vegetation
ACCESS1-0	No	GISS-E2-H-CC	No
ACCESS1-3	No	GISS-E2-R	Yes
BCC-CSM1-1	Yes	GISS-E2-R-CC	No
BCC-CSM1-1-m	Yes	HadGEM2-AO	No
BNU-ESM	No	HadGEM2-CC	Yes
CanESM2	Yes	HadGEM2-ES	Yes
CCSM4	Yes	INMCM4	Yes
CESM1-BGC	Yes	IPSL-CM5A-LR	Yes
CESM1-CAM5	No	IPSL-CM5A-MR	Yes
CMCC-CM	No	IPSL-CM5B-LR	Yes
CMCC-CMS	No	MIROC5	Yes
CNRM-CM5	No	MIROC-ESM	Yes
CSIRO-Mk3-6-0	No	MIROC-ESM-CHEM	Yes
GFDL-ESM2G	Yes	MRI-CGCM3	No
GFDL-ESM2M	Yes	NorESM1-M	Yes
GISS-E2-H	No	NorESM1-ME	Yes

[1] For more information, visit http://cmip-pcmdi.llnl.gov/cmip5/.

Table 3. Names and characteristics of simulations.

Simulation Name	N	Climate (T, P)	Soil Moisture	LAI
Historical	1	Gridded meteorology of Adam and Lettenmaier (2003) and Adam et al. (2006)	Prognostic	MODIS (Myneni et al., 2002)
Warming + Drying + LAI	32	CMIP5 outputs	Prognostic	LAI of corresponding CMIP5 model[1]
Warming + Drying	32	CMIP5 outputs	Prognostic	Historical LAI
Warming + LAI	1	CMIP5 ensemble mean	Historical Asat and WTD from 1981–2010 repeated for 2011–2040, 2041–2070, 2071–2100	Median CMIP5 LAI
Warming	1	CMIP5 ensemble mean	Historical Asat and WTD from 1981–2010 repeated for 2011–2040, 2041–2070, 2071–2100	Historical LAI

[1] For CMIP5 models that did not have a dynamic vegetation component, the median (seasonal cycle, for each grid cell) of the other models' LAI values was used.

Table 4. Names of soil microbial response cases.

Name	Acclimatization	Population shift
NoAcc + NoShift	No	No
Acc + NoShift	Yes	No
Acc + Shift	Yes	Yes

Table 5. End-of-century water- and carbon-cycle terms.

Variable	Units	Soil microbe response	Simulation	Mean WSL	S	N
ET^1_{JJA}	mm H_2O	n/a	Historical	204	238	161
		NoAcc + NoShift	Warming + Drying	243	291	188
			Warming + Drying + LAI	258	305	206
$Asat_{JJA}$	fraction	n/a	Historical	0.462	0.266	0.669
		NoAcc + NoShift	Warming	0.462	0.266	0.669
			Warming + LAI	0.462	0.266	0.669
			Warming + Drying	0.419	0.239	0.622
			Warming + Drying + LAI	0.274	0.158	0.402
WTD_{JJA}	cm	n/a	Historical	17.0	26.1	7.4
		NoAcc + NoShift	Warming	17.0	26.1	7.4
			Warming + LAI	17.0	26.1	7.4
			Warming + Drying	19.7	29.6	8.7
			Warming + Drying + LAI	23.4	34.8	10.5
NPP	$Tg\,C\,yr^{-1}$	n/a	Historical	160	110	50
		NoAcc + NoShift	Warming	199	133	66
			Warming + LAI	237	160	77
			Warming + Drying	220	150	70
			Warming + Drying + LAI	249	162	87
Rh	$Tg\,C\,yr^{-1}$	n/a	Historical	144	100	44
		NoAcc + NoShift	Warming	191	131	60
			Warming + LAI	209	144	65
			Warming + Drying	207	143	64
			Warming + Drying + LAI	221	150	71
CH_4	$Tg\,CH_4\,yr^{-1}$	n/a	Historical	3.36	2.29	1.06
		NoAcc + NoShift	Warming	7.80	5.75	2.05
			Warming + LAI	8.04	5.95	2.09
			Warming + Drying	7.20	5.19	2.01
			Warming + Drying + LAI	6.25	4.24	2.02
		Acc + NoShift	Warming	4.16	2.54	1.61
			Warming + LAI	4.63	2.95	1.68
			Warming + Drying	4.20	2.63	1.57
			Warming + Drying + LAI	3.57	1.97	1.59
		Acc + Shift	Warming	7.79	2.55	5.25
			Warming + LAI	8.48	2.97	5.51
			Warming + Drying	7.92	2.77	5.15
			Warming + Drying + LAI	7.36	2.01	5.36

Table 5. Continued.

Variable	Units	Soil microbe response	Simulation	Mean		
				WSL	S	N
Cnet	$\mathrm{Tg\,C\,yr^{-1}}$	n/a	Historical	−13.5	−8.3	−5.2
		NoAcc + NoShift	Warming	−2.2	2.3	−4.5
			Warming + LAI	−22.0	−11.5	−10.4
			Warming + Drying	−7.6	−3.1	−4.5
			Warming + Drying + LAI	−23.3	−8.8	−14.5
		Acc + NoShift	Warming	−4.9	−0.1	−4.8
			Warming + LAI	−24.5	−13.8	−10.7
			Warming + Drying	−9.9	−5.0	−4.8
			Warming + Drying + LAI	−25.3	−10.5	−14.8
		Acc + Shift	Warming	−2.2	−0.1	−2.1
			Warming + LAI	−21.6	−13.8	−7.9
			Warming + Drying	−7.1	−4.9	−2.1
			Warming + Drying + LAI	−22.5	−10.5	−12.0
GHWP	$\mathrm{Tg\,CO_2\,yr^{-1}}$	n/a	Historical	11.9	11.4	0.3
		NoAcc + NoShift	Warming	134.5	113.4	21.0
			Warming + LAI	66.2	66.3	−0.1
			Warming + Drying	103.5	83.3	20.2
			Warming + Drying + LAI	28.6	45.0	−16.2
		Acc + NoShift	Warming	58.0	46.0	11.8
			Warming + LAI	−5.0	3.5	−8.5
			Warming + Drying	40.5	29.6	11.0
			Warming + Drying + LAI	−27.7	−2.6	−25.3
		Acc + Shift	Warming	134.3	46.2	88.2
			Warming + LAI	75.4	3.7	71.7
			Warming + Drying	118.7	32.5	86.1
			Warming + Drying + LAI	51.9	−1.8	53.9

[1] $\mathrm{ET_{JJA}}$ was not explicitly computed for the Warming and Warming + LAI simulations.

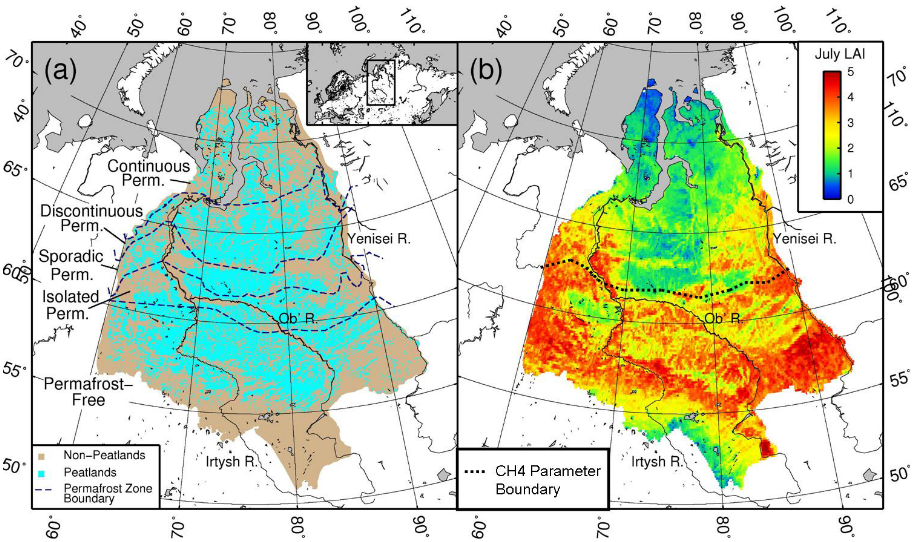

Fig. 1. The West Siberian Lowland (WSL). **(a)** Peatland distribution (from Sheng et al., 2004) and permafrost zone boundaries (after Kremenetski et al., 2003). **(b)** Average July LAI for the period 2003–2010 derived from MODIS (Myneni et al., 2002). Dashed line denotes the boundary between northern and southern CH_4 parameter sets.

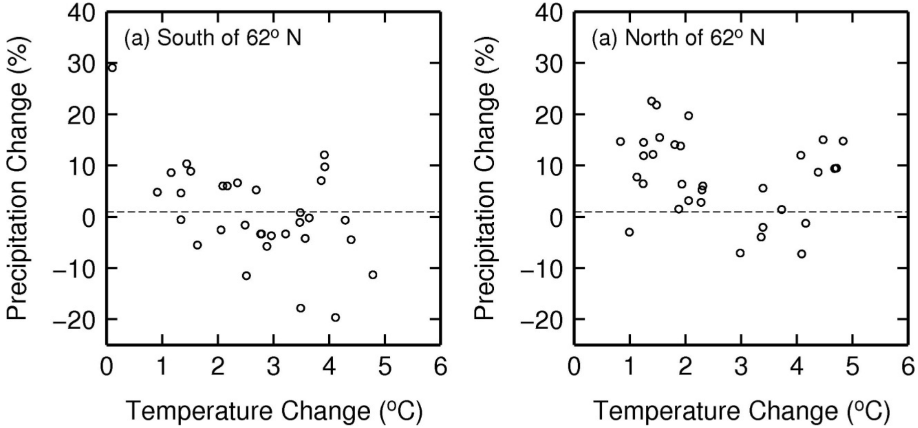

Fig. 2. Differences between end-of-century (2071–2100) and historical (1981–2010) June–August climate given by each of the 32 CMIP5 climate projections, for the West Siberian Lowland, **(a)** south of 62° N, and **(b)** north of 62° N.

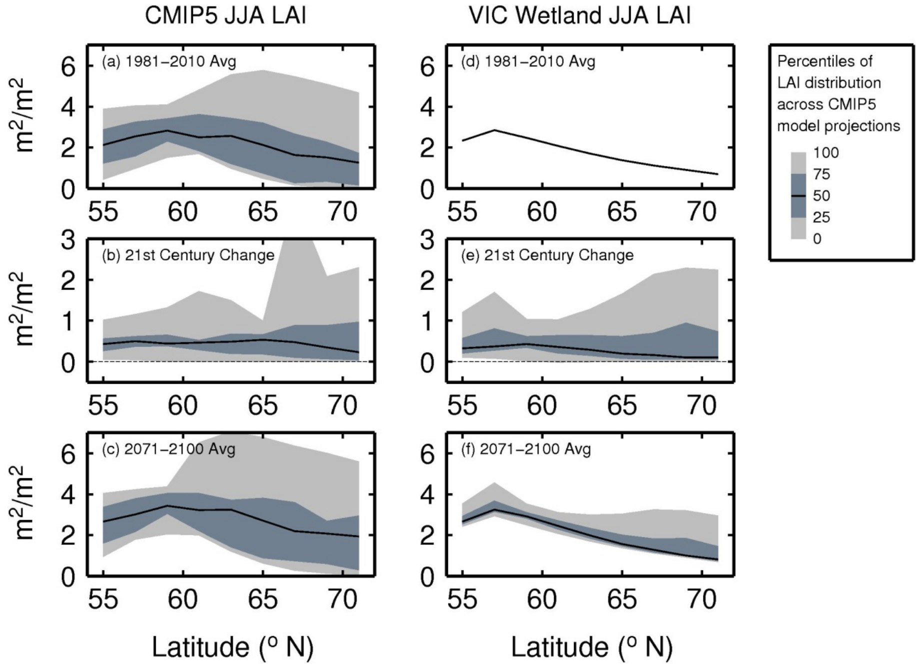

Fig. 3. Distributions of historical and future zonal mean June–August (one-sided) LAI values for CMIP5 models (average LAI over all vegetation types) and VIC simulations (wetland LAI only).

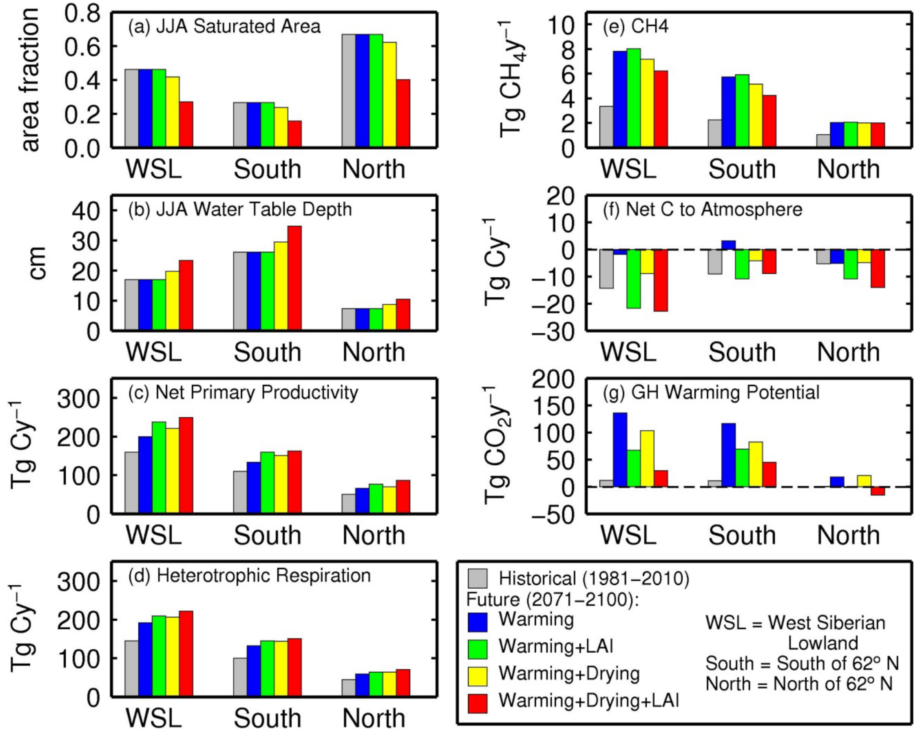

Fig. 4. Simulated historical and end-of-century water and carbon cycle terms over the WSL (average over 32 GCMs) and its southern and northern halves.

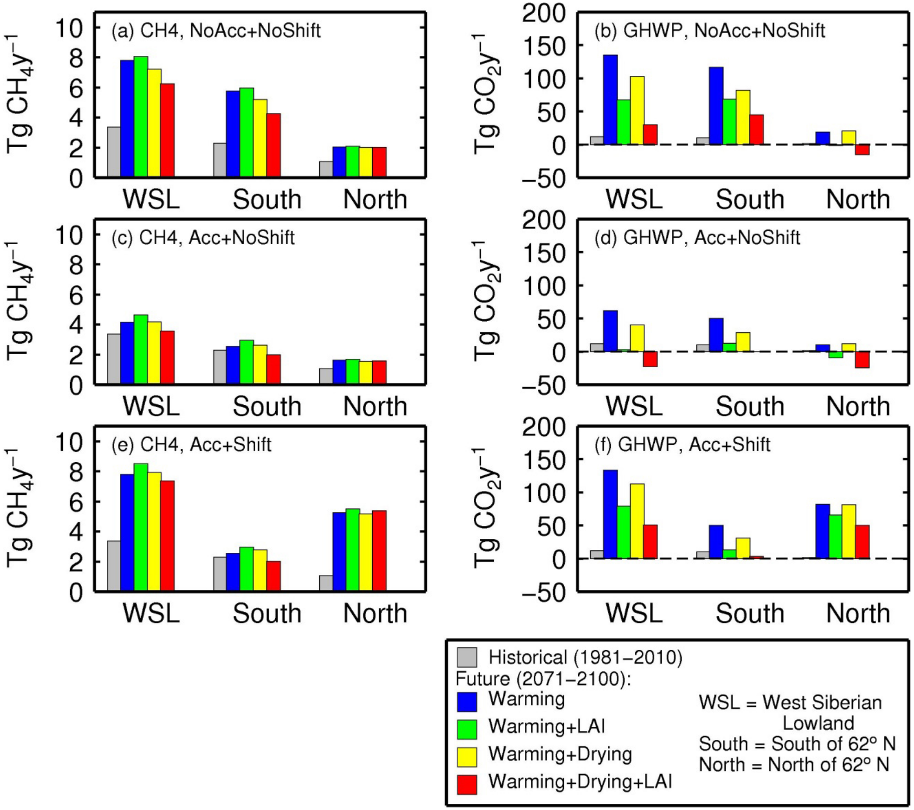

Fig. 5. Simulated historical and end-of-century methane (CH_4) emissions and greenhouse warming potential (GHWP) over the WSL and its southern and northern halves, for the cases of **(a, b)** no acclimatization or population shifts ("NoAcc + NoShift"), **(c, d)** acclimatization but no population shifts ("Acc + NoShift"), and **(e, f)** acclimatization plus population shifts ("Acc + Shift").

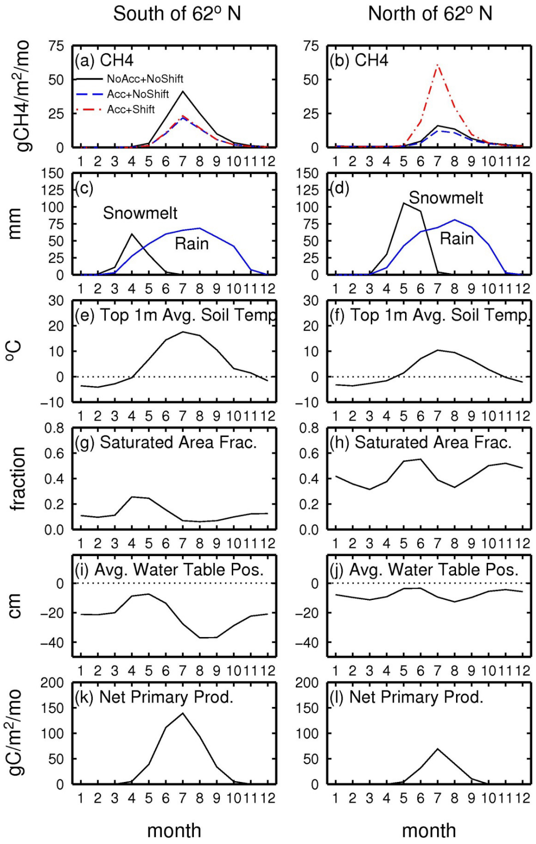

Fig. 6. Monthly spatial average seasonal cycles of methane emissions and hydrologic terms for the period 2071–2100, for the CMIP5 ensemble mean climate forcings and median LAI, for the southern and northern halves of the WSL, for the cases of no acclimatization or population shifts (“NoAcc + NoShift”), acclimatization but no population shifts (“Acc + NoShift”), and acclimatization plus population shifts (“Acc + Shift”).